

Single and double photoionization of beryllium below 40 eV

R. Wehlitz,^{1,*} D. Lukić,² and J. B. Bluett¹

¹*Synchrotron Radiation Center, UW-Madison, Stoughton, Wisconsin 53589, USA*

²*Institute of Physics, 11001 Belgrade, Serbia and Montenegro*

(Received 21 July 2004; published 10 January 2005)

We have measured the double-to-single photoionization ratio of beryllium ($1s^2 2s^2$) between 28 and 40 eV and determined the relative single- and double-photoionization cross sections. In this energy region only *simultaneous* but not sequential emission of both $2s$ electrons can take place. We also compare our data with recent theoretical calculations and find good agreement with our data. The previously found scaling law for the double-to-single photoionization ratio is confirmed with high accuracy.

DOI: 10.1103/PhysRevA.71.012707

PACS number(s): 32.80.Fb

I. INTRODUCTION

Helium has long been used as a test bench system for probing electron correlations, and agreement between experiments and theories has greatly improved over the years (see, e.g., [1,2]). Following helium, beryllium ($1s^2 2s^2$) is the most important closed-shell atom which is simple enough to be calculated by *ab initio* methods which now become available. The double-photoionization process in other alkaline earths, such as Ba [3], Ca [4–6], and Sr [7], has attracted attention recently. However, Be is the simplest alkaline earth and has the advantage that from its first double-ionization threshold (27.534 eV [8]) up to about 115 eV autoionization (or Auger) processes cannot contribute to the double-photoionization cross section.

One interesting difference of the double-photoionization process between He and Be is the much lower binding energy of both valence electrons, which in Be is only 9.3 eV as opposed to 24.6 eV in He. Thus, the double-ionization threshold is much lower as compared to He (79.0 eV). Also, doubly ionized Be, unlike He, has two remaining electrons and many-body effects may have an influence on the energy dependence of the double-photoionization cross section.

Stimulated by these interesting properties, experimental investigations of the double-photoionization process in Be have begun recently [9–11] despite the experimental challenges. The first measurement of the double-to-single photoionization ratio [9] has rather large error bars so that a comparison with theoretical calculations and numerical models was a less stringent test. Here, we present further data for the relative double-photoionization cross sections and the corresponding double-to-single photoionization ratio from threshold up to 40 eV. We have also measured the relative single-photoionization cross section from 20 to 40 eV photon energy. The data have significantly smaller error bars as compared to previous measurements [9]. Some of the low-energy data presented here have been analyzed regarding the near-threshold behavior of the double-photoionization cross section [11].

The first calculation for the double-to-single photoionization ratio in Be was done by Berrington *et al.* [12] who

calculated a ratio of about 4% below the K -shell excitations at 115 eV using the R -matrix method. More recent calculations using the convergent close-coupling (CCC) method [13], the time-dependent close-coupling method (TDCC) [14], and the hyperspherical R -matrix method with semiclassical outgoing waves (HRM-SOW) [15] also became available. Other calculations on Be concentrate on the total cross section for the higher [12] and lower [16] photon energies or focus on autoionization features below the double-ionization threshold [17,18] or on the K -shell region above 115 eV [19–21].

II. EXPERIMENT

The experiment was performed at the 4-m normal-incidence monochromator beamline [22] of the Synchrotron Radiation Center (SRC). The photons were monochromatized by a 1200-lines/mm Al-MgF₂ grating and entered the experimental chamber through a glass capillary. The photon-energy resolution was about 30 meV at 28 eV. The photon beam intersected the Be vapor emerging from a resistively heated oven. The temperature of the tantalum crucible was typically 1150 °C to vaporize Be wire. This temperature yields an estimated Be vapor pressure of 10^{-5} mbar [23] whereas the background pressure in the vacuum chamber was about 2×10^{-8} mbar during the experiment. The surface of the Be wire was mechanically cleaned to remove the oxide layer. The crucible inside the grounded and water-cooled cooling jacket was biased by 5 V to avoid thermal electrons from leaking into the interaction region.

The Be ions created in the interaction region were extracted by a pulsed electrical field of 20 V/cm across the interaction region. The pulses had a period of 12.5 μ s and a width of 1.4 μ s. The ions were accelerated into a drift tube, and detected by a Z-stack microchannel-plate detector operated at 3000 V. The preamplified ($\times 10$) multichannel plate (MCP) pulse was processed by a constant-fraction discriminator (CFD). The threshold of the CFD was set to a sufficiently low level (150 mV) to ensure that there was no difference in the detection efficiency between the singly and doubly charged ions. The threshold was determined experimentally by measuring the Be⁺ and Be²⁺ count rates as a function of the CFD threshold. We also measured the count

*Electronic address: wehlitz@src.wisc.edu

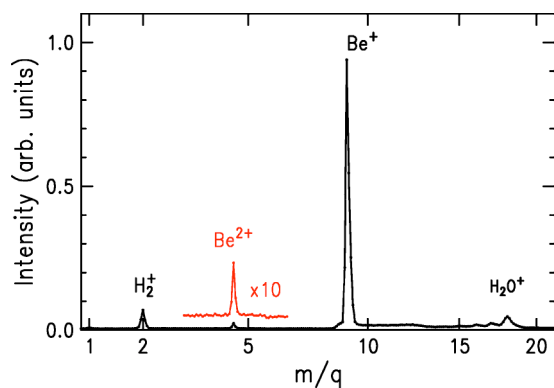


FIG. 1. Partial ion-yield spectrum of Be taken at $h\nu=37.0$ eV. The region around the Be^{2+} peak is multiplied by 10 for clarity. Note that the abscissa has a nonlinear scale of the mass-to-charge ratio.

rates as a function of the MCP voltage on the front side of the MCP assembly. The count rates for both charge states leveled off at around 3000 V.

By measuring the ions' flight time we obtained the singly and doubly charged ion yields of Be. A typical ion yield spectrum taken at 37.0 eV photon energy is shown in Fig. 1. This spectrum is not background corrected and shows besides the Be ion peaks a small contamination of water.

The beam of Be atoms was trapped on a liquid-nitrogen-cooled copper foil. The incident photon flux was monitored with a nickel mesh. An ion-yield scan across the Ar $3s \rightarrow np$ resonances between 26 and 29 eV served as a convenient photon energy calibration. Other details of the setup can be found elsewhere [24].

We did not employ any filters since the photon flux of this normal-incident monochromator naturally decreases quickly above ~ 35 eV and second-order light does not play a role here.

III. DATA ANALYSIS

In order to determine the photon-energy dependence of the double-to-single photoionization ratio of Be, we took ion time-of-flight spectra at several photon energies. The areas of the Be^+ and Be^{2+} ion peaks were numerically integrated.

We applied an energy correction to the photon energy, which we determined by taking an ion-yield scan across the Ar $3s \rightarrow np$ resonances, which have well-known energies [25]. We found an offset in wavelength of 0.253 \AA . The energy correction was assumed to be a constant shift in wavelength over the energy range of interest, resulting in an energy offset of, e.g., 18 meV at 30 eV.

IV. RESULTS AND DISCUSSION

A. Double-to-single photoionization ratio

From the measured Be^+ and Be^{2+} ion yields we determined the double-to-single photoionization ratios between 28 and 40 eV photon energy, which are shown in Fig. 2 along with previously measured ratios [9]. The theoretical ratios using the convergent close-coupling calculation of

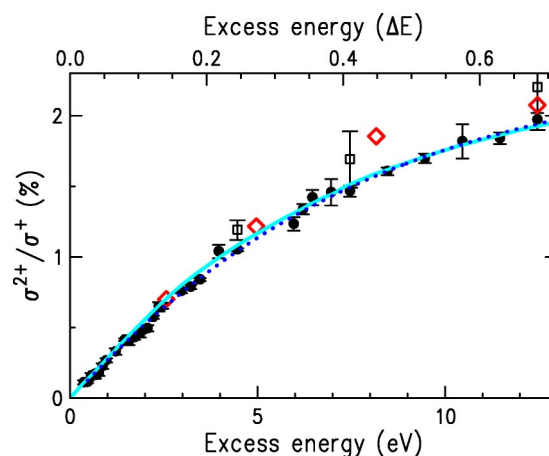


FIG. 2. Double-to-single photoionization ratio of Be as a function of excess energy (filled circles, this work; open squares, [9]). The open diamonds are calculated values from Kheifets and Bray [13]. The solid line is the He double-to-single photoionization ratio [26] multiplied by 0.636 on an energy scale in units ΔE of the difference between the double- and single-ionization thresholds. The dotted line (partly overlapping with the solid line) is a fit to our data using a universal shape function [27].

Kheifets and Bray [13] are in accord with our data, although their point at 8-eV excess energy seems to be too large. We have also plotted in Fig. 2 the double-to-single photoionization ratio of He [26] multiplied by 0.636 on an energy scale that is in units of the corresponding energy difference between the double- and single-ionization thresholds ΔE . For Be the energy unit ΔE is $27.5 - 9.3 = 18.2$ eV while for He ΔE is $79.0 - 24.6 = 54.4$ eV. This scaling was successfully applied [9,28] to He, Li, Be, and H_2 . Our improved Be data show an excellent agreement with the scaled He data and clearly confirm this scaling law.

A possible explanation why our energy scaling works so well may be found in the similarity between electron-impact ionization and double photoionization [29] and in a scaling law for electron-impact ionization [30]. Samson [29] discovered that the double-to-total photoionization ratio of an atom is proportional to the electron-impact ionization cross section of the corresponding ion. Since the double-to-single photoionization ratio is small, the double-to-total photoionization ratio is approximately the same as the double-to-single photoionization ratio. Now, the single-ionization cross section σ_e by electron impact for the hydrogen isoelectronic sequence is a function of the incident electron energy E divided by the ionization potential I , i.e., $\sigma_e = F(E/I)$ [see Eq. (4) in [30]]. In the case of single ionization of a singly charged ion, the corresponding ionization potential is then the double-ionization potential (since we end up with a doubly charged ion) minus the single-ionization potential (since we have an already singly ionized target). As a result of combining the proportionality found by Samson and the scaling law for electron-impact ionization, one may expect some similarity between the double-to-single photoionization ratios of different targets if the energy axis is given in units of the energy difference between the double- and single-ionization thresholds. However, it is not clear why the energy

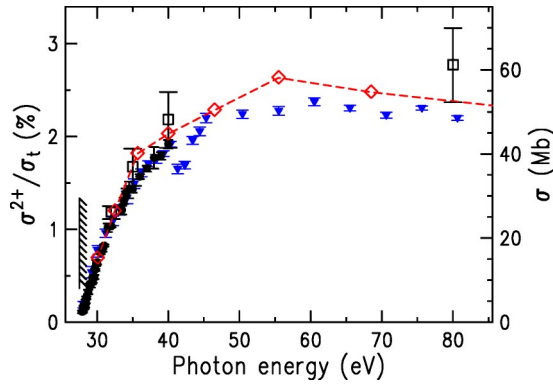


FIG. 3. The double-to-total photoionization ratio of Be (left-hand scale) as a function of photon energy (filled circles) together with previous measurements [9] (open squares) compared with the total cross section (right-hand scale) of electron-impact ionization of Be^+ (filled triangles) [33]. The diamonds connected by a dashed line are the calculated double-to-total photoionization ratios of Kheifets and Bray [13].

scaling works so surprisingly well. Nevertheless, the fact that the scaling works so well indicates that the mechanism of the double-photoionization process is the same for all atoms.

Noteworthy is also the excellent fit of a universal shape function introduced by Pattard [27] which is shown as a dotted line in Fig. 2. This shape function for the double-to-single photoionization ratio is based on a previously proposed shape function for ionization by bare projectiles [31]. As described in Ref. [27], basically the universal shape function connects the low-energy behavior, given by the Wannier theory [32], with the high-energy behavior as given by the Bethe-Born theory. The formula used to fit our ratios is [27]

$$\frac{\sigma^{2+}}{\sigma^+}(E) = R_\infty \frac{E^\alpha (E + E_0)^{7/2}}{(E + E_1)^{(\alpha+7/2)}}. \quad (1)$$

For the case of double photoionization $\alpha=1.056$. R_∞ is the asymptotic high-energy double-photoionization ratio, and E_0 and E_1 are fit parameters. We have used the theoretical value for $R_\infty=0.3709\%$ [13] and obtained for $E_0=136.7$ eV and $E_1=47.2$ eV the fit curve shown in Fig. 2. Since the data extend only over a small energy range the fit parameters may be slightly different if data become available for a larger energy range. We have also used R_∞ as a fit parameter and obtained a value of $0.08(66)\%$ indicating that data at higher photon energies are needed if one wants to determine the asymptotic high-energy ratio.

In order to compare our data with the electron-impact cross section for Be^+ we converted the double-to-single photoionization ratio to a double-to-total photoionization ratio. As Samson has pointed out [29], this conversion is necessary for a correct comparison of the electron-impact ionization data and double-photoionization data. As can be seen in Fig. 3, we find a good agreement between our ratios and the normalized electron-impact data of Be^+ . Please note that the electron-impact data are shifted by the binding energy of the $2s$ electron (9.323 eV [8]). The proportionality of electron-impact ionization of a singly charged ion to the

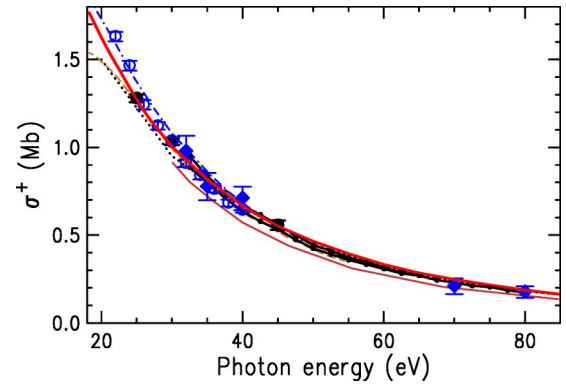


FIG. 4. Relative single-photoionization cross section of Be compared with theoretical calculations; dotted line, R -matrix calculation [12]; dash-dotted line, relativistic random-phase approximation (RRPA) [17]; dashed line, multi-configuration relativistic random-phase approximation (MCRRPA) [17]; thick solid line, Hartree-Fock-Slater calculation [35]; thin solid line, CCC calculation [13]; solid line with dots, HRM-SOW in L , V , and A gauge [15]. Our data points (open and filled circles) were derived by different methods and scaled to fit the curve of Yeh and Lindau [35]. The diamonds are data from Wehlitz and Whitfield [9].

double photoionization of the same neutral atom was found previously for several atoms (He, Ne, Ar, N, O) and explained by Samson [29].

B. Relative single-photoionization cross section

In order to determine the relative single-photoionization cross section we took several spectra between 22 and 45 eV photon energy. The collection time was rather short (ca. 300 s) to ensure an as constant as possible Be vapor pressure during this measurement. For a direct comparison, we leaked some Ne gas into the chamber in addition to the Be vapor. From the known Ne^+ cross section [34] we directly calculated the relative Be^+ cross section. By using this method, it is not necessary to monitor the photon flux. The resulting Be^+ cross section is shown in Fig. 4 as filled circles. However, the Ne gas reacted with the hot heating filament, which burnt within a short period of time.

Therefore, we repeated this measurement in two steps. First, we determined the relative yield curve of a Ni mesh mounted just upstream of the beamline's exit flange using the Ne^+ cross sections of Bizau and Wuilleumier [34]. Note that those Ne^+ cross sections are averaged values of previous measurements. By measuring the photocurrent of the Ni mesh and applying our Ni yield curve, we were able to monitor the relative photon flux while taking Be spectra. These cross section data are shown as open circles in Fig. 4 along with calculated cross section curves [12,13,17,35]. The cross section of the experimental data is scaled so that the data fit the curve of Yeh and Lindau [35]. Overall, we find a fair agreement of our data with the energy dependence of the calculated cross sections. Only the MCRRPA curve of Chi *et al.* [17] and R -matrix curve of Berrington *et al.* [12] seem to bend down at lower energies while our data show a slight increase of the cross section relative to the theoretical curves.

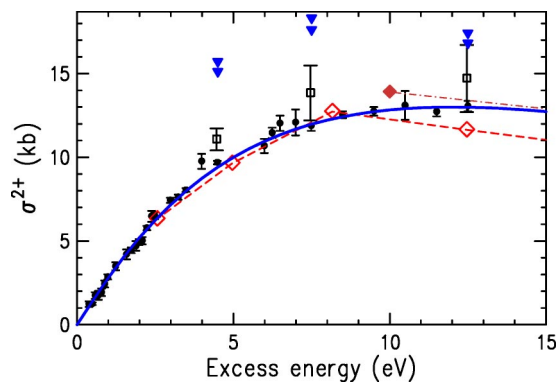


FIG. 5. Relative double-photoionization cross section as a function of excess energy (filled circles). Previous measurement [9] (open squares), CCC calculations [13] (open diamonds), TDCC calculations [14] (filled diamond), and HRM-SOW calculations in the L , V , and A gauges [15] (triangles). The solid line is a fit to our data using a universal shape function [27].

We need to point out that our data depend on an accurate Ne^+ cross section. While we have used the Ne^+ cross section data of Bizau and Wuilleumier [34], the data of Wuilleumier and Krause [36] and Marr and West [37] give very similar results within our error bars. The data of Henke *et al.* [38], however, result in an artificial bump in the Be^+ cross section at low energies (not shown).

C. Relative double-photoionization cross section

Using our double-to-single photoionization ratios and the single-ionization cross section of Yeh and Lindau [35] we derived the relative double photoionization cross section which is shown in Fig. 5. The absolute scale is only an approximation since it is based on the theoretical Be^+ cross section. As one can see in Fig. 4 the cross sections from different calculations vary by up to 10%. Nevertheless, the agreement of our relative double photoionization cross section with the calculations of Kheifets and Bray [13] as well as Colgan and Pindzola [14] is remarkably good whereas the calculation of Citrini *et al.* [15] is slightly higher than our data.

Again we applied an universal shape function, but this time for the double photoionization cross section [27], which is shown as a solid line in Fig. 5. The formula for the multiple photoionization cross section $\sigma(E)$ is given by [27]

$$\sigma(E) = \sigma_M x^\alpha \left(\frac{\alpha + 7/2}{\alpha x + 7/2} \right)^{\alpha+7/2}, \quad (2)$$

with $\alpha=1.056$, $x=E/E_M$, and E_M and σ_M the position and height of the cross section maximum, respectively; i.e., σ_M

$=\sigma(E_M)$. Only the two parameters σ_M and E_M are used to fit the model function to the experimental data. We have used $\sigma_M=13$ kb and $E_M=12$ eV for the curve shown in Fig. 5.

V. SUMMARY

In conclusion, we have measured the relative single-photoionization cross section between 22 and 45 eV and the double-to-single photoionization ratio of Be between 28 and 40 eV in small energy steps. We have found good agreement of this ratio with the theoretical calculations of Kheifets and Bray [13]. We also found remarkable agreement between the photon-energy dependence of the double-to-single photoionization ratio of Be and He [26] using appropriately scaled data. While this scaling model has been seen before [9] our additional data provide strong evidence in support of this model. The model function used here resembles those model functions which are applied to electron-impact ionization cross sections and may allow predictions of the double-to-single photoionization ratio for other systems.

Furthermore, we confirm that the double-to-total photoionization ratio shows the same energy dependence as the normalized electron-impact cross section of Be^+ [33] based on a model introduced by Samson [29].

The relative single-photoionization cross section agrees well with theoretical calculations [12,13,17,35] with a slight advantage for the RRP curve of Chi *et al.* [17] at energies below 27 eV.

The double-photoionization cross section agrees very well with the calculated cross sections of Kheifets and Bray [13] and Colgan and Pindzola [14]. A universal shape function developed by Pattard [27] provides an excellent fit curve to our data.

Future measurements of the single- and double-photoionization cross sections of Be just below the K edge are desirable but are challenging due to possible second-order light with energies above the K edge. This enables Auger decay processes to take place, which overwhelmingly contribute to the creation of doubly charged ions, so that even a small amount of second-order light will disturb the measurements.

ACKNOWLEDGMENTS

The authors wish to thank the staff of the Synchrotron Radiation Center for their excellent support. One of us (D.L.) was partly supported by the Ministry of Science, Technology and Development of Serbia. This work was partly supported by the National Science Foundation (NSF) under Grant No. PHY-9987638 and is based upon research conducted at the SRC, University of Wisconsin-Madison, which is supported by the NSF under Award No. DMR-0084402.

- [1] I. Bray, D. V. Fursa, A. S. Kheifets, and A. T. Stelbovics, *J. Phys. B* **35**, R117 (2002), and references therein.
- [2] J. H. McGuire, N. Berrah, R. J. Bartlett, J. A. R. Samson, J. A. Tanis, C. L. Cocke, and A. S. Schlachter, *J. Phys. B* **28** 913 (1995), and references therein.
- [3] D. M. P. Holland and K. Codling, *J. Phys. B* **13**, L293 (1980).
- [4] L. Malegat, F. Citrini, P. Selles, and P. Archirel, *J. Phys. B* **33**, 2409 (2000).
- [5] F. Maulbetsch, I. L. Cooper, and A. S. Dickinson, *J. Phys. B* **33**, L119 (2000).
- [6] H.-J. Beyer, J. B. West, K. J. Ross, and A. De Fanis, *J. Phys. B* **33**, L767 (2000).
- [7] J. B. West, K. J. Ross, H. J. Beyer, A. De Fanis, and H. Hamdy, in 13th International Conference on Vacuum Ultraviolet Physics, Trieste, Italy, 2001 (unpublished).
- [8] A. A. Radzig and B. M. Smirnov, *Reference Data on Atoms, Molecules, and Ions* (Springer-Verlag, Berlin, 1985); *Phys. Rev. Lett.* **59**, 2736 (1987).
- [9] R. Wehlitz and S. B. Whitfield, *J. Phys. B* **34**, L719 (2001).
- [10] S. Hasegawa, S. Obara, F. Yoshida, T. Suzuki, Y. Azuma, and T. Nagata, in *International Workshop on Photoionization* (SPRING-8, Hyogo, Japan, 2002), p. FA17.
- [11] D. Lukić, J. B. Bluett, and R. Wehlitz, *Phys. Rev. Lett.* **93**, 023003 (2004).
- [12] K. Berrington, L. Quigley, and H. L. Zhang, *J. Phys. B* **30** 5409 (1997).
- [13] A. S. Kheifets and I. Bray, *Phys. Rev. A* **65**, 012710 (2001).
- [14] J. Colgan and M. S. Pindzola, *Phys. Rev. A* **65**, 022709 (2002).
- [15] F. Citrini, L. Malegat, P. Selles, and A. K. Kazansky, *Phys. Rev. A* **67**, 042709 (2003).
- [16] D.-S. Kim, S. S. Tayal, H.-L. Zhou, and S. T. Manson, *Phys. Rev. A* **61**, 062701 (2000).
- [17] H.-C. Chi, K.-N. Huang, and K. T. Cheng, *Phys. Rev. A* **43**, 2542 (1991).
- [18] B. Zhou and C. D. Lin, *Phys. Rev. A* **51**, 1286 (1995).
- [19] L. VoKy, H. E. Saraph, W. Eissner, Z. W. Liu, and H. P. Kelly, *Phys. Rev. A* **46**, 3945 (1992).
- [20] M. Kutzner, D. Winn, and S. Mattingly *Phys. Rev. A* **48** 404 (1993).
- [21] E. W. B. Dias, H. S. Chakraborty, P. C. Deshmukh, and S. T. Manson, *J. Phys. B* **32**, 3383 (1999).
- [22] C. H. Pruett, E. L. Brodsky, R. K. Cole, S. L. Crossley, D. B. Crossley, R. W. C. Hansen, T. Nelson, F. K. Perkins, G. C. Rogers, R. A. Rosenberg, D. J. Wallace, W. R. Winter, F. H. Middleton, A. Filipponi, and F. Zanini, *Rev. Sci. Instrum.* **60**, 1913 (1989).
- [23] R. E. Honig and D. A. Kramer, *RCA Rev.* **30**, 285 (1969).
- [24] R. Wehlitz, D. Lukić, C. Koncz, and I. A. Sellin, *Rev. Sci. Instrum.* **73**, 1671 (2002).
- [25] S. L. Sorensen, T. Åberg, J. Tulkki, E. Rachlew-Källne, G. Sundström, and M. Kirm, *Phys. Rev. A* **50**, 1218 (1994).
- [26] J. A. R. Samson, W. C. Stolte, Z.-X. He, J. N. Cutler, Y. Lu, and R. J. Bartlett, *Phys. Rev. A* **57**, 1906 (1998).
- [27] T. Pattard, *J. Phys. B* **35**, L207 (2002).
- [28] R. Wehlitz, J. B. Bluett, and S. B. Whitfield, *Phys. Rev. A* **66**, 012701 (2002).
- [29] J. A. R. Samson, *Phys. Rev. Lett.* **65**, 2861 (1990).
- [30] K. Aichele, U. Hartenfeller, D. Hathiramani, G. Hofmann, V. Schäfer, M. Steidl, M. Stenke, E. Salzborn, T. Pattard, and J. M. Rost, *J. Phys. B* **31**, 2369 (1998).
- [31] J. M. Rost and T. Pattard, *Phys. Rev. A* **55**, R5 (1997).
- [32] G. Wannier, *Phys. Rev.* **90**, 817 (1953).
- [33] R. A. Falk and G. H. Dunn, *Phys. Rev. A* **27**, 754 (1983).
- [34] J. M. Bizau and F. J. Wuilleumier, *J. Electron Spectrosc. Relat. Phenom.* **71**, 205 (1995).
- [35] J. J. Yeh and I. Lindau, *At. Data Nucl. Data Tables* **32**, 1 (1985).
- [36] F. Wuilleumier and M. O. Krause, *J. Electron Spectrosc. Relat. Phenom.* **15**, 15 (1979).
- [37] G. V. Marr and J. B. West, *At. Data Nucl. Data Tables* **18**, 497 (1976).
- [38] B. L. Henke, E. M. Gullikson, and J. C. Davis, *At. Data Nucl. Data Tables* **54**, 181 (1993).